

Article

Not peer-reviewed version

Efficient analysis of small molecules via laser desorption/ionization time-of-flight mass spectrometry (LDI-TOF MS) using gold nanoshells with nanogaps

Noori Kim, [Yoon-Hee Kim](#), Jin Yoo, [Seung-min Park](#), [Bong-Hyun Jun](#)*, [Woon-Seok Yeo](#)*

Posted Date: 24 August 2023

doi: [10.20944/preprints202308.1675.v1](https://doi.org/10.20944/preprints202308.1675.v1)

Keywords: Matrix-assisted laser desorption/ionization time-of-flight mass spectrometry; gold nanoshell; nanogap; surface-assisted laser desorption/ionization; silica core nanoparticle; small-molecule analysis.



Preprints.org is a free multidiscipline platform providing preprint service that is dedicated to making early versions of research outputs permanently available and citable. Preprints posted at Preprints.org appear in Web of Science, Crossref, Google Scholar, Scilit, Europe PMC.

Copyright: This is an open access article distributed under the Creative Commons Attribution License which permits unrestricted use, distribution, and reproduction in any medium, provided the original work is properly cited.

Disclaimer/Publisher's Note: The statements, opinions, and data contained in all publications are solely those of the individual author(s) and contributor(s) and not of MDPI and/or the editor(s). MDPI and/or the editor(s) disclaim responsibility for any injury to people or property resulting from any ideas, methods, instructions, or products referred to in the content.

Article

Efficient Analysis of Small Molecules via Laser Desorption/Ionization Time-of-Flight Mass Spectrometry (LDI-TOF MS) Using Gold Nanoshells with Nanogaps

Noori Kim ^{1,†}, Yoon-Hee Kim ^{1,†}, Jin Yoo ¹, Seung-min Park ², Bong-Hyun Jun ^{1,*} and Woon-Seok Yeo ^{1,*}

¹ Department of Bioscience and Biotechnology, Konkuk University, Seoul 05029, Republic of Korea; bobbyesen@naver.com (N. Kim); yoonhees@konkuk.ac.kr (Y.-H. Kim); jin4261624@gmail.com (J. Yoo)

² Department of Urology, Stanford University School of Medicine, Stanford, 94305, United States; sp293@stanford.edu (S.-M. Park)

* Correspondence: bjun@konkuk.ac.kr (B.-H. Jun); wsyeo@konkuk.ac.kr (W.-S. Yeo)

† N. Kim and Y.-H. Kim contributed equally to this work.

Abstract: Matrix-assisted laser desorption/ionization time-of-flight mass spectrometry (MALDI-TOF MS) is a commonly used technique for analyzing large biomolecules. However, the utilization of organic matrices limits the small-molecule analysis because of the interferences in the low-mass region and reproducibility issues. To overcome these limitations, a surface-assisted laser desorption/ionization (SALDI), which utilizes nanostructured metallic surfaces, has been developed. Herein, a novel approach for SALDI-MS was proposed using nanoengineered gold shell with nanogaps on the silica core ($\text{SiO}_2@\text{Au}$ NGS), which is an emerging material due to its excellent heat-generating capabilities. The gold shell thickness was controlled by adjusting the concentration of gold precursor for the growth of gold nanoparticles. SALDI-MS measurements were performed on a layer formed by drop-casting a mixture of $\text{SiO}_2@\text{Au}$ NGS and analytes. At the optimized process, the gold shell thickness was observed to be 17.2 nm, which showed the highest absorbance. The ion desorption efficiency was confirmed with a survival yield upon fragmentation. Based on the enhanced SALDI capability, $\text{SiO}_2@\text{Au}$ NGS was utilized to detect various small molecules including amino acids, sugars, and flavonoids. The limits of detection, reproducibility, and salt tolerance of $\text{SiO}_2@\text{Au}$ NGS demonstrate its potential as an effective and reliable SALDI material for small-molecule analyses.

Keywords: Matrix-assisted laser desorption/ionization time-of-flight mass spectrometry; gold nanoshell; nanogap; surface-assisted laser desorption/ionization; silica core nanoparticle; small-molecule analysis

1. Introduction

Matrix-assisted laser desorption/ionization time-of-flight (MALDI-TOF) mass spectrometry (MS) is widely used for the analysis of large biomolecules, such as proteins and oligonucleotides, using an organic matrix for soft ionization.[1-3] Following the pioneering studies of Tanaka et al., who utilized a metal powder dispersed in glycerol,[4,5] and Karas and Hillenkamp, who employed a small organic molecule as a matrix,[6] various types of organic matrices, including 2,5-dihydroxybenzoic acid, sinapinic acid, α -cyano-4-hydroxycinnamic acid, and 2,4,6-trihydroxyacetophenone, are commonly used for this purpose depending on the analyte type. MALDI-TOF MS is an effective bioanalytical tool for biomolecules because of its simple and fast operating processes, high tolerance to biological contaminants, and the ability to facilitate multiple analyses simultaneously. However, the necessity of the use of an organic matrix considerably limits its practical application (particularly for small-molecule analyses) because of the interferences in the low-mass region. In addition, the solvents utilized for dissolving the analyte and matrix, the co-crystallization of the matrix and analyte, and even the deposition method strongly affect the shot-to-

shot and sample-to-sample reproducibility of this technique. To overcome these limitations, significant efforts have been devoted to develop an organic matrix-free analysis method known as surface-assisted laser desorption/ionization (SALDI), which is primarily based on the use of nanostructured surfaces and inorganic nanoparticles (NPs) instead of the organic matrix.[7,8]

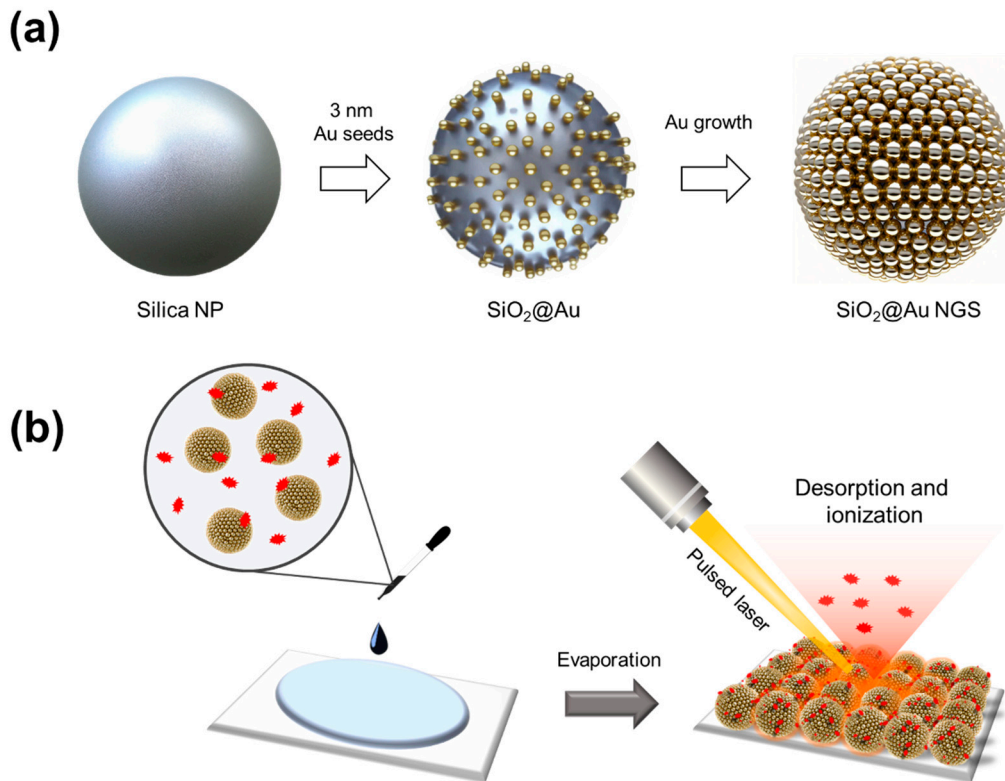
Since the pioneering study of Tanaka, who employed 30 nm cobalt NPs dispersed in glycerol for lysozyme analysis,[5] various nanomaterials based on metals, including Au, Ag, TiO₂, Zn, and Pt, have been applied for SALDI-MS.[9] Furthermore, carbon-based materials, such as graphite, carbon nanotubes, graphene oxide (GO), and graphene derivatives, have been actively used for this purpose.[10-12] In particular, inorganic NPs, including gold nanoparticles (AuNPs)[13] and silver NPs,[14] are widely employed in SALDI-MS because of their advantageous physiochemical properties, photothermal activities, and simple fabrication procedures affording homogeneously controllable morphologies; however, these NPs easily dissipate heat owing to their high thermal conductivity. Several attempts have been conducted to obtain efficient SALDI substrates by confining the laser-driven energy to nanoscale gap structures. As a result, substrates with closely packed nanostructures fabricated via vapor deposition [15] and droplet deposition [16] were produced. The SALDI efficiency and signal strength of these substrates strongly correlated with their sub-micrometer and nanometer-scale morphologies, which could be controlled by adjusting the sputtered metal amount and number of deposition cycles. However, fabricating homogeneous nanogap structures via these methods is difficult owing to the bulk agglomerate formation and uncontrolled interparticle aggregation during the deposition process.

Recently, “gold nanoshells,” core-shell NPs consisting of silica NP cores and AuNP surfaces were utilized for the first time as a SALDI substrate by Jinrui et al.[17] Such materials can effectively confine heat by the silica core NPs and abundant “hot spots” distributed across the interparticle junctions of the closely packed AuNPs on the silica surface. The existence of correlations between the SALDI signals of various analytes and thickness of gold nanoshells was discussed in detail by Mingyi et al.[18] They prepared three types of gold nanoshells and compared their SALDI efficiencies, which depended on the surface coverage and shell roughness at the nanometer scale. The optimized gold nanoshells with the highest SALDI efficiency have been successfully applied in the mass spectrometry imaging of the mouse brain. In these applications, gold nanogap structures generated “hot spots,” which consisted of the highly localized regions of an intense electromagnetic field due to plasmonic coupling between adjacent nanostructures. Recently, we have prepared gold nanogap shells using silica NPs, which significantly amplified a local electromagnetic field.[19,20] Finely controlled nanogap structures were obtained by increasing the shell thickness, which in turn decreased the average nanogap size from approximately 4 to 1 nm. Although these NPs were utilized as substrates and catalysts for surface-enhanced Raman scattering spectroscopy, they have not been employed for SALDI yet.

Herein, we propose an organic matrix-free LDI-MS method using nanoengineered gold shells with nanogaps supported on the silica surface (SiO₂@Au NGS). SiO₂@Au NGS with various shell thicknesses and well-ordered surface structures were synthesized by modulating the Au precursor concentration during growth (Scheme 1a). To utilize the prepared SiO₂@Au NGS as a matrix for LDI-TOF spectrometry (Scheme 1b), a layer of SiO₂@Au NGS was formed by drop-casting a mixture of colloidal SiO₂@Au NGS and target analytes. Desorption and ionization of these analytes were performed by irradiating the resulting layer with a pulsed laser beam.

2. Experimental Section

2.1. Chemicals



Scheme 1. Schematics of the (a) $\text{SiO}_2@\text{Au}$ NGS preparation through the seed-mediated growth, and (b) detection of target analytes via the $\text{SiO}_2@\text{Au}$ NGS-assisted LDI technique.

Quercetin hydrate, cellobiose, triethylene glycol, tetraethylene glycol, tetraethyl orthosilicate (TEOS), gold(III) chloride, polyvinylpyrrolidone (PVP, average molecular weight: $\sim 10,000$), (3-aminopropyl)trimethoxysilane (APTS), and ascorbic acid were purchased from Sigma–Aldrich (St. Louis, MO, USA). Glutamic acid, mannitol, serine, galactose, histidine, and aqueous ammonium hydroxide (NH_4OH , 25–28%) were procured from Daejung Chemical & Metals Co., Ltd. (Gyeonggi-do, Korea). Aspartic acid and acetonitrile were acquired from Junsei Chemical Co., Ltd. (Tokyo, Japan). Kaempferol hydrate and pentaethylene glycol were purchased from Tokyo Chemical Industry (Tokyo, Japan). Tryptophan, arginine, and glutamine were procured from Samchun Chemicals Co., Ltd. (Gyeonggi-do, Korea). Absolute ethanol was obtained from Merck (Darmstadt, Germany). GO was purchased from Graphene Laboratories Inc. (Ronkonkoma, NY, USA). Benzyl pyridinium salt was prepared using a method previously reported by Tang et al.[21] Deionized water was obtained using an AquaMAX Ultra 370 water purification system (Younglin Instruments, Anyang, Korea).

2.2. Synthesis of $\text{SiO}_2@\text{Au}$ NGS

AuNPs were prepared using tetrakis(hydroxymethyl)phosphonium chloride (THPC) as a reducing agent. First, a NaOH solution (0.2 M, 1.5 mL) was diluted with deionized water (47.5 mL), followed by the sequential addition of THPC (80%, 12 μL) and gold(III) chloride (50 mM, 1 mL) solutions. The obtained mixture was vigorously stirred for 1 h. AuNP-seed-immobilized silica NPs ($\text{SiO}_2@\text{Au}$) were synthesized using a silica NP template. Silica NPs were prepared via the Stöber process.[22] Briefly, TEOS (1.6 mL) was mixed with ethanol (40 mL), followed by the addition of the NH_4OH solution (3–5.5 mL) to obtain silica NPs of various sizes. The reaction mixture was stirred vigorously for 1 h at 60°C and then for 19 h at 25°C. The produced solution was washed several times with ethanol via centrifugation at 9000 $\times g$. The resulting silica NPs (15 mg) were modified with amino groups by stirring with the APTS (15.5 μL) and NH_4OH (10 μL) solutions in a vortex mixer for 12 h. The mixture was washed several times with ethanol via centrifugation at 9000 $\times g$, and the obtained

minated silica NPs (2 mg) were mixed with the AuNP solution (10 mL) overnight. After washing with deionized water, the resulting dark-brown pellets were dispersed in ethanol. $\text{SiO}_2@\text{Au}$ NGS were synthesized through the seed-mediated growth of $\text{SiO}_2@\text{Au}$ at different concentrations of the gold precursor solution. Briefly, $\text{SiO}_2@\text{Au}$ (10 mg) was dispersed in an aqueous PVP solution and stirred at 500 rpm. During stirring, 200 μL of a 50 mM Au^{3+} aqueous solution and 100 mM ascorbic acid aqueous solution were added simultaneously at 5 min intervals. The addition of the precursor solutions was repeated to achieve a final Au^{3+} concentration of 0.5, 1.0, 1.5, or 2 mM. The obtained mixture was washed several times with deionized water and redispersed in ethanol. The resulting $\text{SiO}_2@\text{Au}$ NGS_{0.5-2.0} dispersions were stored in a refrigerator.

2.3. Characterization

Transmission electron microscopy (TEM) images were captured using JEM-1010 (JEOL, Tokyo, Japan) and JEM-2010 (JEOL, Tokyo, Japan) instruments with acceleration voltages of 80 and 120 kV, respectively. The UV-visible absorption spectra were recorded using a single-beam UV/visible spectrophotometer (U-5100, HITACHI, Tokyo, Japan).

2.4. MALDI-TOF MS analysis of small molecules

To prepare the samples for LDI-TOF MS analyses, 100 μM stock solutions of small molecules were produced. The amino acids and sugars were dissolved in distilled water, and oligoethylene glycols and flavonoids were dissolved in ethanol. $\text{SiO}_2@\text{Au}$ NGS_{0.5-2.0} (10 μL , 1 mg/mL in ethanol) were mixed with the analyte solutions (5 μL) at various concentrations, and the obtained mixtures (1.5 μL) were pipetted onto stainless-steel 384-well target plates (Bruker Daltonics, Germany). The prepared samples were dried under vacuum at 25°C and analyzed directly via MS. The MALDI-TOF MS analyses were performed using an Autoflex III MALDI-TOF mass spectrometer (Bruker Daltonics, Germany) equipped with a smart beam laser serving as an ionization source. All spectra were acquired in a positive mode at an accelerating voltage of 19 kV and repetition rate of 50 Hz with an average number of shots equal to ~500.

3. Results and Discussions

3.1. Preparation and characterization of $\text{SiO}_2@\text{Au}$ NGS

The fabrication process of $\text{SiO}_2@\text{Au}$ NGS is illustrated in Scheme 1a. $\text{SiO}_2@\text{Au}$ NGS was synthesized in two steps, including the attachment of AuNP seeds to silica NPs and seed-mediated growth of AuNP seeds. To attach AuNPs to the substrate surface, silica NPs (~178 nm) were aminated with APTS. Then, the aminated silica NPs were mixed with AuNPs (~3 nm) to prepare the AuNP seed-immobilized silica NPs. Subsequently, gold precursor solutions with different concentrations were added to grow AuNP seeds, resulting in $\text{SiO}_2@\text{Au}$ NGS. The $\text{SiO}_2@\text{Au}$ NGS morphology was controlled by varying the concentration of the Au^{3+} precursor in the reaction mixture during the growth process, as shown in the corresponding transmission electron microscopy (TEM) images (Figure 1a-f). The size of AuNPs that constitute the outer gold shell depended on the concentration of the Au^{3+} precursor, which was varied as 0, 0.5, 1.0, 1.5 and 2.0 mM, resulting in different shell thicknesses of 2.3, 8.3, 11.9, 13.1 and 17.2 nm ($\text{SiO}_2@\text{Au}$ NGS_{0.5-2.0}). Notably, the shell thickness affected not only the nanogap size but also plasmonic absorption properties. Characteristic plasmonic frequencies of the $\text{SiO}_2@\text{Au}$ NGS with different Au^{3+} concentrations were observed in their absorption spectra recorded in the ultraviolet (UV)/visible range (Figure S1). To evaluate the laser irradiation absorption properties of various $\text{SiO}_2@\text{Au}$ NGS samples during LDI, their absorbances at 355 nm are compared in Figure 1f. The absorbance gradually increases with increasing Au^{3+} concentration from 0 to 1.5 mM, and a slight increase in absorbance is observed at 2.0 mM. These structural and optical characteristics can be used to predict the desorption efficiency during LDI spectrometry using the laser-driven energy for the desorption and ionization of analytes.

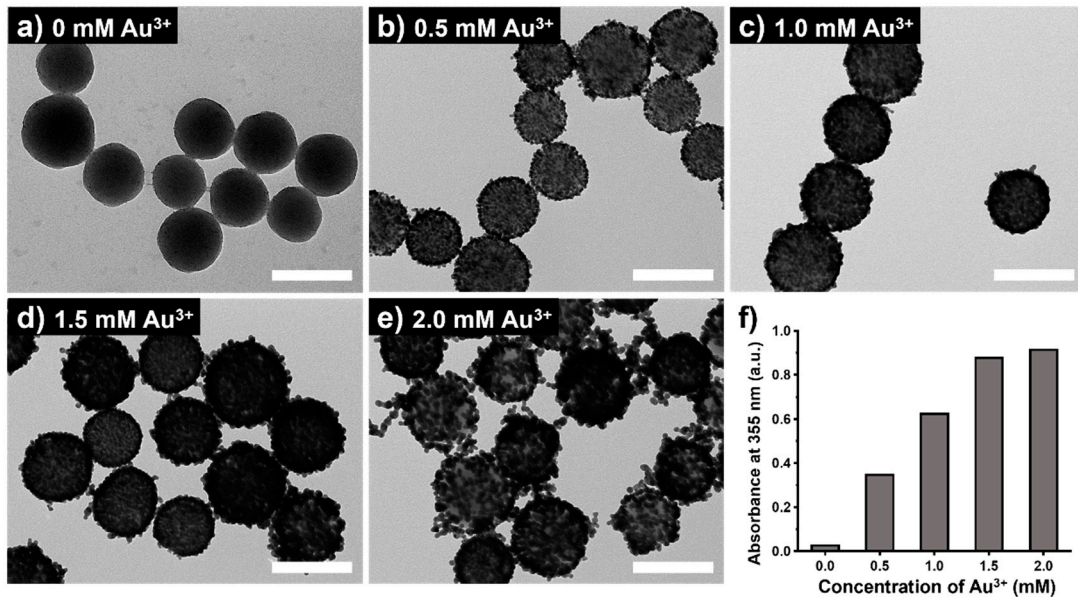


Figure 1. TEM images of SiO₂@Au NGS obtained after the growth of AuNP seeds at gold precursor concentrations of (a) 0, (b) 0.5, (c) 1.0, (d) 1.5, and (e) 2.0 mM. (f) Absorption values at 355 nm correspond to each SiO₂@Au NGS. Inset scale bars of (a–e) indicate 200 nm.

3.2. Matrix properties of SiO₂@Au NGS_{0.5–2.0} evaluated using small molecules

We examined the feasibility of utilizing SiO₂@Au NGS_{0.5–2.0} as matrices for LDI–TOF MS analysis and their efficiency by studying various small molecules including amino acid serine, sugar mannitol, quercetin, and pentaethylene glycol. The analytes were dissolved in distilled water or ethanol, considering their solubility differences, and the resulting solutions were mixed with the synthesized SiO₂@Au NGS_{0.5}, SiO₂@Au NGS_{1.0}, SiO₂@Au NGS_{1.5}, and SiO₂@Au NGS_{2.0}. AuNP seed-immobilized silica NPs (SiO₂@Au NGS₀) produced without seed-mediated gold growth were used as a control. Five representative mass spectra recorded for each of the four analytes are shown in Figure 2, and their detailed peak assignments and peak intensities are summarized in Table S1. In general, the molecular ion peaks corresponding to the studied analytes are clearly observed in Figure 2, and their intensities increase with increasing concentration of the gold precursor solution during the SiO₂@Au NGS synthesis. Except while using quercetin, the peak intensities of SiO₂@Au NGS_{2.0} are significantly higher than those of the other SiO₂@Au NGS — by a factor of 4 for serine, 25 for mannitol, and 10 for pentaethylene glycol. We presumed that the surface area of the embedded gold shell nanostructures with nanogaps on the silica surface increased with increasing gold precursor concentration to facilitate the accommodation of the energy supplied by laser irradiation and its subsequent transfer to the analytes, which increased the SALDI efficiency. In addition, the enhanced plasmonic properties of SiO₂@Au NGS and rapid heating due to the low thermal conductivity of the silica NP core significantly enhanced the SALDI effect. In summary, SiO₂@Au NGS_{2.0} exhibited the optimal matrix properties among the four gold shell materials, and we further validated the versatility of this material for LDI–MS by analyzing various small molecules and comparing it with other well-known SALDI materials.

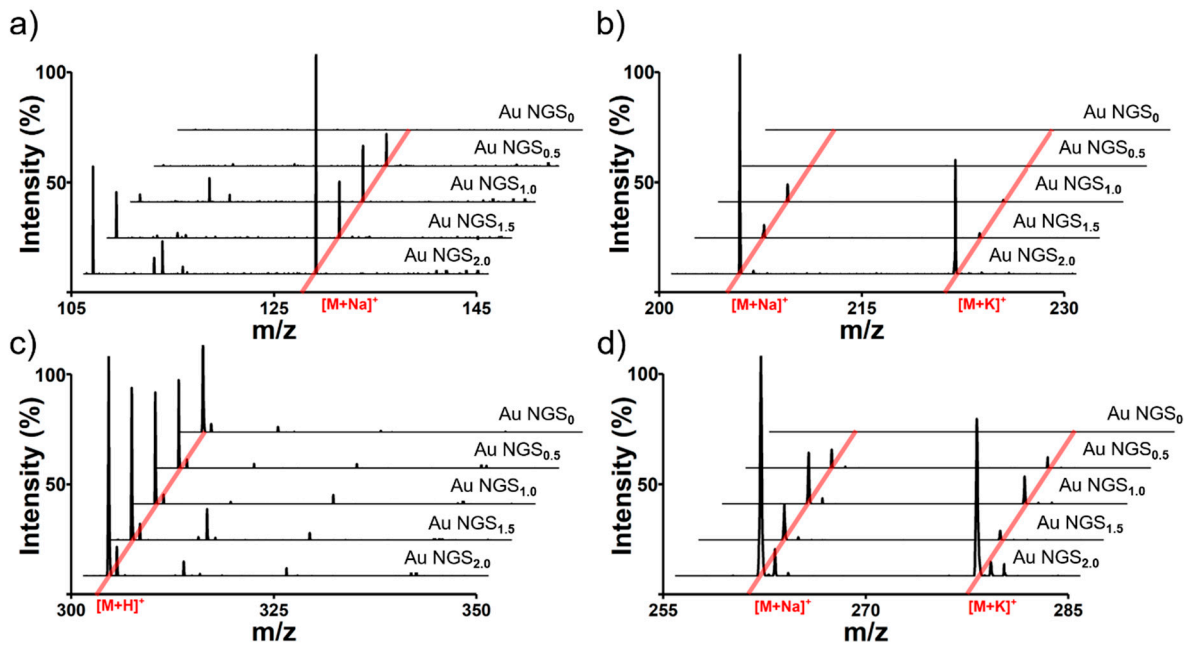


Figure 2. LDI-TOF mass spectra of small molecules obtained for the $\text{SiO}_2@\text{Au NGS}_{0-2.0}$ matrices: (a) serine, (b) mannitol, (c) quercetin, and (d) pentaethylene glycol.

3.3. Analyses of small molecules and their mixtures

Next, we analyzed various small molecules using $\text{SiO}_2@\text{Au NGS}_{2.0}$ to evaluate the matrix properties of the synthesized material. Four classes of small molecules were examined: amino acids (aspartic acid, glutamic acid, and glutamine), oligoethylene glycols (triethylene glycol and tetraethylene glycol), sugars (mannitol and galactose), and flavonoids (quercetin and kaempferol). Analytical solutions for LDI-MS analysis were prepared using distilled water for amino acids and sugars and ethanol for oligoethylene glycols and flavonoids. As shown in Figure 3, the SALDI spectra of $\text{SiO}_2@\text{Au NGS}_{2.0}$ exhibit distinct strong peaks corresponding to the molecular ions of amino acids (a–c), oligoethylene glycols (d, e), sugars (f, g), and flavonoids (h, i) with high intensities and signal-to-noise (S/N) ratios without any significant background interferences (detailed peak assignment is provided in Table S2). A gold peak is observed at $m/z = 196.97$. Subsequently, mixtures of small molecules were tested to confirm the separation of each analyte from the mixed samples. We prepared mixed samples containing three amino acids (glutamine, histidine, and arginine), three oligoethylene glycols (triethylene glycol, tetraethylene glycol, and pentaethylene glycol), three sugars (galactose, mannitol, and cellobiose), and three molecules from different classes (tryptophan, quercetin, and cellobiose). The mass spectra of each analyte mixture also clearly show major peaks corresponding to the molecular ions of the studied analytes with weak background peaks (Figure 4; for detailed peak assignment, see Table S3). These results strongly suggest that the nanoengineered gold shells with nanogaps on the silica surface $\text{SiO}_2@\text{Au NGS}_{2.0}$ with well-ordered surface structures is a highly effective SALDI material for the analysis of various small molecules and their mixtures.

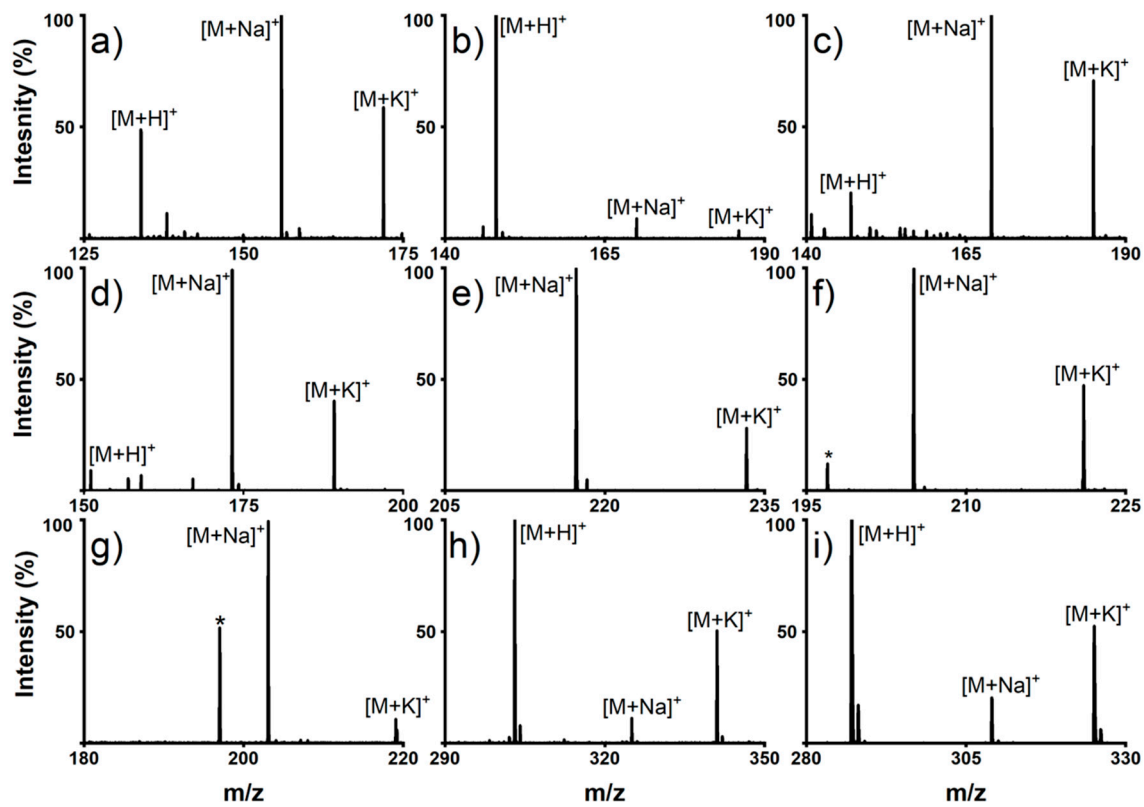


Figure 3. LDI-TOF mass spectra of amino acids: ((a) aspartic acid, (b) glutamic acid, and (c) glutamine); oligoethylene glycols: ((d) triethylene glycol and (e) tetraethylene glycol); sugars: ((f) mannitol and (g) galactose); and flavonoids: ((h) quercetin and (i) kaempferol) obtained using the $\text{SiO}_2@\text{Au}$ $\text{NGS}_{2.0}$ matrix. *: matrix.

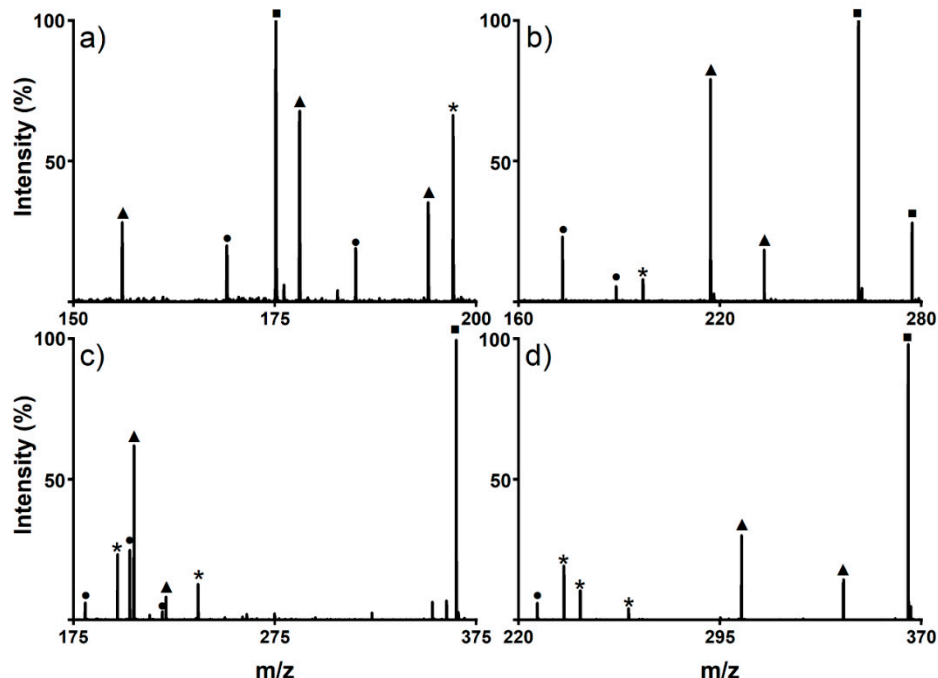


Figure 4. LDI-TOF mass spectra obtained for the mixtures of (a) amino acids (●: Glutamine, ▲: histidine, and ■: arginine), (b) oligoethylene glycols (●: triethylene glycol, ▲: tetraethylene glycol,

and ■: pentaethylene glycol), (c) sugars (●: galactose, ▲: mannitol, and ■: cellobiose), and d) sugar (●: tryptophan, ▲: quercetin, and ■: cellobiose) using the $\text{SiO}_2@\text{Au}$ NGS_{2.0} matrix. *: matrix.

3.4. Comparison of AuNP, GO, and $\text{SiO}_2@\text{Au}$ NGS matrices

The superiority of $\text{SiO}_2@\text{Au}$ NGS_{2.0} as a SALDI matrix over other commonly used inorganic matrices, AuNPs and GO was verified by comparing their SALDI properties using four analytes: kaempferol, cellobiose, triethylene glycol, and serine. As shown in Figure 5, the mass spectra obtained for $\text{SiO}_2@\text{Au}$ NGS_{2.0} are more distinct than those recorded for AuNPs and GO. The GO spectrum exhibited kaempferol peaks with the highest intensity compared to the intensities of three compounds but with very poor resolution, whereas the other three analytes were negligibly observed. Both AuNPs and $\text{SiO}_2@\text{Au}$ NGS_{2.0} generated most intense analyte peaks; however, $\text{SiO}_2@\text{Au}$ NGS_{2.0} exhibited high peak intensities and resolution.

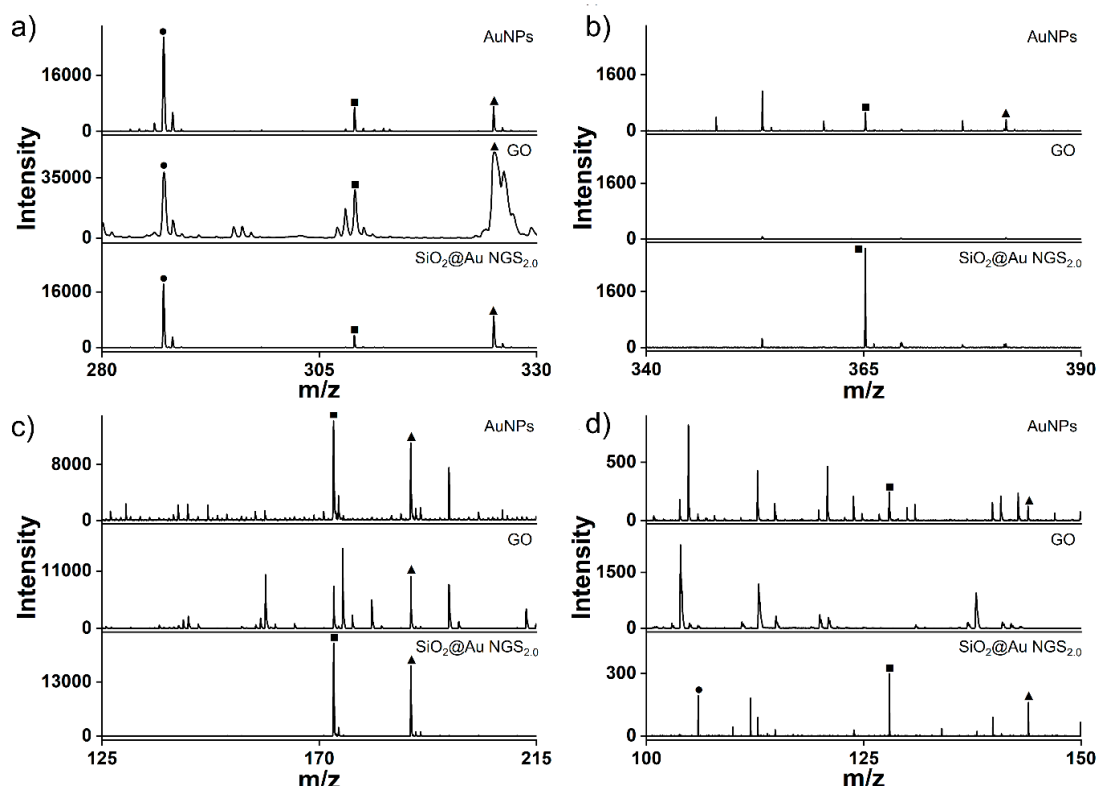


Figure 5. LDI-TOF mass spectra of small molecules obtained using the AuNP, GO, and $\text{SiO}_2@\text{Au}$ NGS_{2.0} matrices: (a) kaempferol, (b) cellobiose, (c) triethylene glycol, and (d) serine. ●: $[\text{M}+\text{H}]^+$, ■: $[\text{M}+\text{Na}]^+$, and ▲: $[\text{M}+\text{K}]^+$.

Furthermore, we examined the applicability of $\text{SiO}_2@\text{Au}$ NGS_{2.0} as a SALDI matrix using benzylpyridinium (BP) salt, which has been adopted as a “chemical thermometer” to investigate the ion desorption efficiency and internal energy transfer by measuring a survival yield (SY).[21] BP is fragmented via laser irradiation during the LDI process to produce benzylic carbocations (Figure 6a); therefore, the SY of BP is an important parameter characterizing the SALDI efficiency and ionization “softness.” The SY was calculated by dividing the ion intensity of the intact BP precursor by the sum of the intact BP and fragmented product intensities after LDI-MS measurements. Five SALDI analyses were conducted for BP using AuNPs, GO, and $\text{SiO}_2@\text{Au}$ NGS_{2.0} under the same experimental conditions. The obtained representative spectra are shown in Figure 6b. The average SY values determined from the five mass spectra were 0.63 for AuNPs, 0.41 for GO, and 0.64 for $\text{SiO}_2@\text{Au}$ NGS_{2.0}. These results indicate that $\text{SiO}_2@\text{Au}$ NGS_{2.0} exhibits excellent SALDI matrix properties during small-molecule analysis.

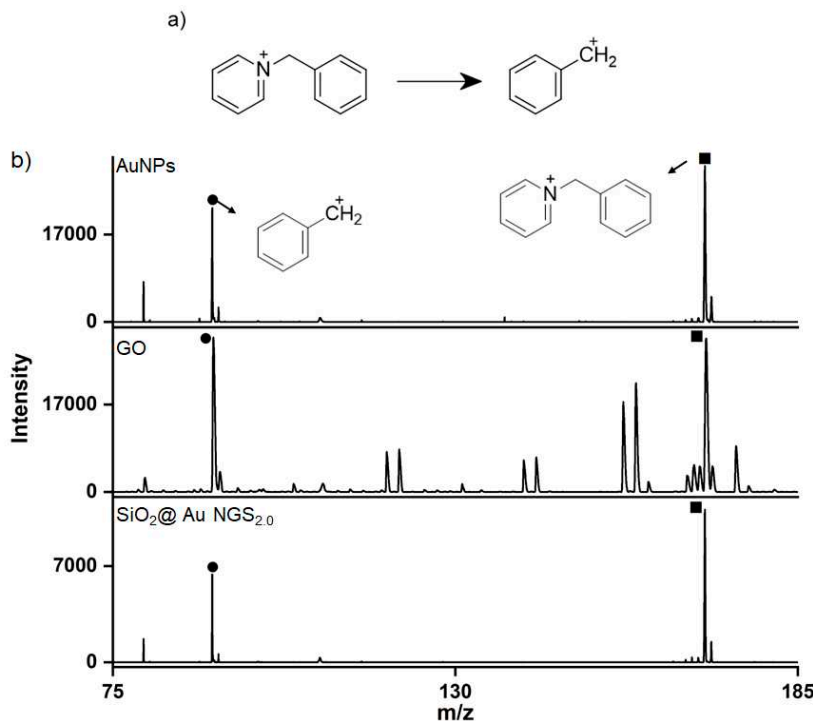


Figure 6. LDI-TOF mass spectra recorded during BP analysis. (a) Fragmentation reaction of BP during LDI-TOF measurements, and (b) representative LDI-TOF mass spectra obtained using the AuNP, GO, and $\text{SiO}_2@\text{Au NGS}_{2.0}$ matrices. ●: Fragment and ■: BP.

3.5. Limits of detection (LODs), reproducibility, and salt tolerance

LODs were measured for three analytes (glutamine, cellobiose, and kaempferol) to evaluate the practical feasibility of the $\text{SiO}_2@\text{Au NGS}_{2.0}$ -based LDI technique. The LODs obtained at S/N ratios higher than six were 37.5 pmole for glutamine, 7.5 fmole for cellobiose, and 75 fmole for kaempferol (Figure 7). These values are comparable to those determined in previous studies using gold-based materials.[13,23] We also investigated the reproducibility of the fabricated material via multiple mass determinations ($n = 25$) for cellobiose (100 pmole in 1 μL on the target plate). The calculated relative standard deviation of 18.6% was comparable to or better than the values obtained in other studies using AuNPs (Figure S2).[24] Another major issue encountered during MALDI analysis is the signal suppression for analytes with salt contaminants (typically, 150 mM NaCl).[25] Because SALDI materials are tolerant to high salt concentrations,[26] we tested two analytes, histidine and mannitol, to investigate the salt tolerance of $\text{SiO}_2@\text{Au NGS}_{2.0}$. The analytes were prepared in NaCl solutions at concentrations ranging from 0.1 to 1 M and then examined using $\text{SiO}_2@\text{Au NGS}_{2.0}$. The SALDI spectra of histidine clearly show the main peaks of the sodium adduct ($[\text{M}+\text{Na}]^+$) at $m/z = 178.01$ and two sodium adducts ($[\text{M}+2\text{Na}-\text{H}]^+$) at $m/z = 200.01$ (Figure 8a). For mannitol, a sodium adduct peak ($m/z = 205.01$, $[\text{M}+\text{Na}]^+$) was observed as the main peak with a trace potassium adduct ($[\text{M}+\text{K}]^+$) and two sodium adduct peaks (Figure 8b). For both analytes, $\text{SiO}_2@\text{Au NGS}_{2.0}$ generated molecular ion peaks as the main peaks at NaCl concentrations up to 1 M, indicating a high salt tolerance of the SALDI material; however, the peak intensities decreased with increasing salt concentration.

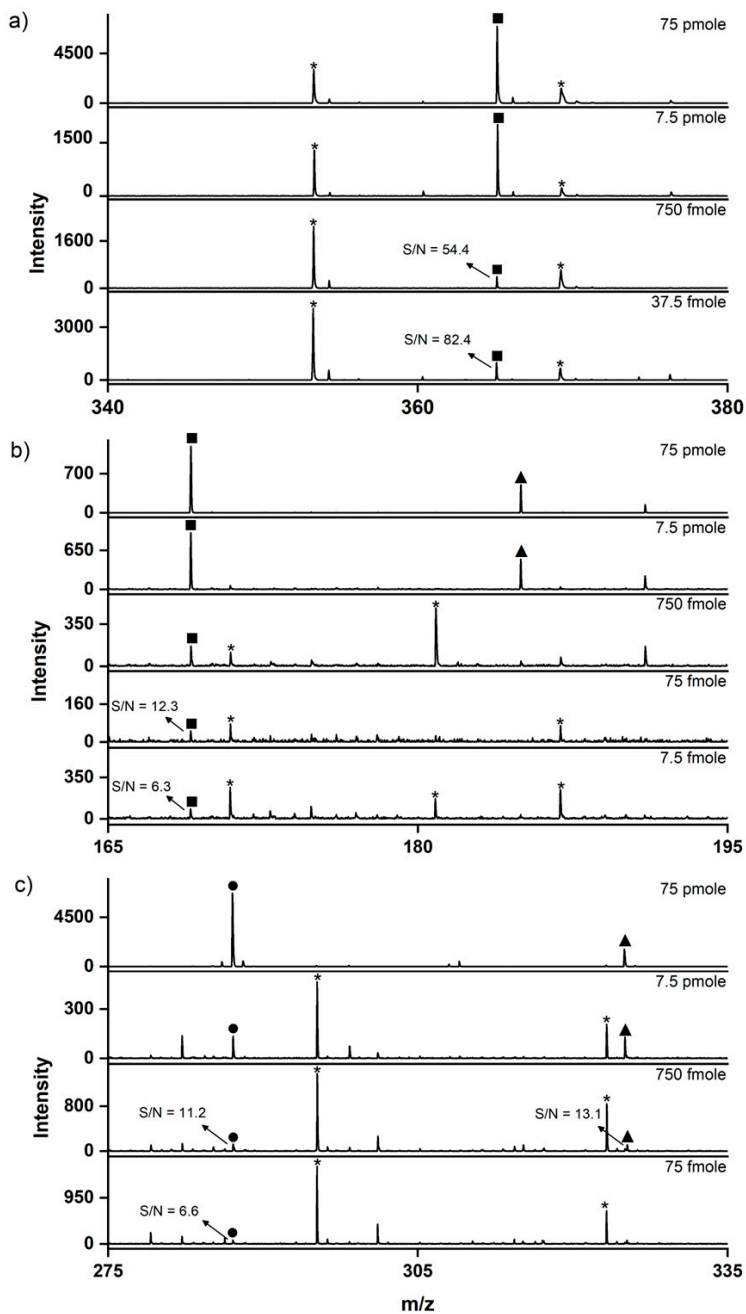


Figure 7. LDI-TOF mass spectra recorded to determine the LODs of small molecules using the $\text{SiO}_2@\text{Au}$ NGS_{2.0} matrix: **(a)** glutamine, **(b)** cellobiose, and **(c)** kaempferol. ●: $[\text{M}+\text{H}]^+$, ■: $[\text{M}+\text{Na}]^+$, ▲: $[\text{M}+\text{K}]^+$, and *: matrix.

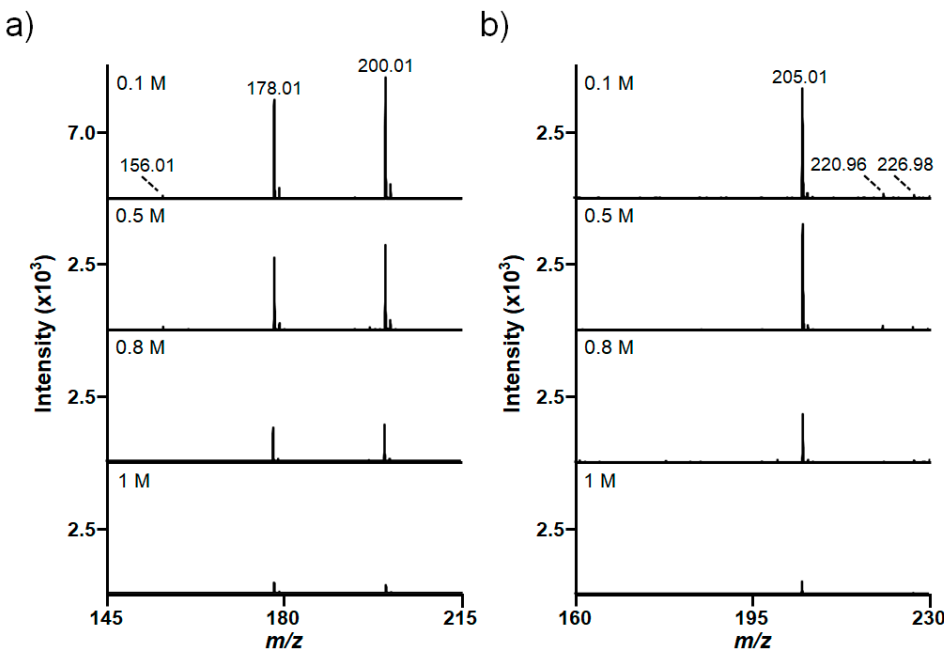


Figure 8. Salt tolerance of the $\text{SiO}_2@\text{Au}$ NGS_{2.0} matrix. Studied analytes (1 mM) were mixed with the NaCl solutions of various concentrations ranging between 0.1 and 1 M. (a) Histidine ($m/z = 178.01$, $[\text{M}+\text{Na}]^+$ and $m/z = 200.01$, $[\text{M}+2\text{Na}-\text{H}]^{2+}$). (b) Mannitol ($m/z = 205.01$, $[\text{M}+\text{Na}]^+$; $m/z = 220.96$, $[\text{M}+\text{K}]^+$; and $m/z = 226.98$, $[\text{M}+2\text{Na}-\text{H}]^{2+}$).

4. Conclusions

In summary, nanoengineered gold shells with nanogaps on the silica surface were utilized for the SALDI-MS analysis of small molecules. As the gold shell thickness increased, the plasmonic absorption of the $\text{SiO}_2@\text{Au}$ NGS increased gradually, while maintaining its well-ordered nanogap structure. In addition, the signal intensity and S/N ratio of the SALDI-MS peaks also exhibited a similar correlation with the gold shell thickness of $\text{SiO}_2@\text{Au}$ NGS. The phenomenon is presumed to be because of the high UV absorbance, which is advantageous for the heat-generation contributing to the desorption of the analyte. Based on the excellent SALDI performance of $\text{SiO}_2@\text{Au}$ NGS_{2.0}, various small molecules including amino acids, sugars, flavonoids, and their mixtures were investigated. This material demonstrated high reproducibility and salt tolerance, and its LODs were comparable to or better than those of other SALDI materials. Therefore, the material fabricated in this study can potentially replace the matrix-free LDI-MS analytical tools currently used by researchers.

Supplementary Materials: The following supporting information can be downloaded at: Preprints.org, Figure S1: Absorption spectra of $\text{SiO}_2@\text{Au}$ NGS; Figure S2: Signal variation of cellobiose; Table S1: Detailed peak assignments for mass spectra in Figure 2; Table S2: Detailed peak assignments for mass spectra in Figure 3; Table S3: Detailed peak assignments for mass spectra in Figure 4

Author Contributions: Conceptualization, B.-H. Jun and W.-S. Yeo; methodology, Y.-H. Kim and J. Yoo; software, N. Kim and Y.-H. Kim; validation, S.-M Park, B.-H. Jun and W.-S. Yeo; formal analysis, N. Kim and Y.-H. Kim; investigation, N. Kim, Y.-H. Kim and J. Yoo; resources, N. Kim and Y.-H. Kim; data curation, N. Kim and Y.-H. Kim; writing—original draft preparation, N. Kim and Y.-H. Kim; writing—review and editing, S.-M. Park, B.-H. Jun and W.-S. Yeo; visualization, Y.-H. Kim; supervision, B.-H. Jun and W.-S. Yeo; project administration, B.-H. Jun and W.-S. Yeo; funding acquisition, B.-H. Jun and W.-S. Yeo. All authors have read and agreed to the published version of the manuscript.

Funding: This research was supported by the National Research Foundation of Korea (NRF) funded by the Korean government (MSIT) [grant number NRF-2022R1A2C1006152], Ministry of Science and ICT [grant number NRF-2022R1A2C2012883], and Ministry of Trade, Industry, and Energy (MOTIE) of the Republic of Korea [grant number 20018608].

Data Availability Statement: The data presented in this study are available on request from the corresponding author.

Conflicts of Interest: The authors declare no conflict of interest.

References

1. Hale, J.E.; Butler, J.P.; Knierman, M.D.; Becker, G.W. Increased Sensitivity of Tryptic Peptide Detection by MALDI-TOF Mass Spectrometry Is Achieved by Conversion of Lysine to Homoarginine. *Anal Biochem* **2000**, *287*, 110–117, doi:10.1006/abio.2000.4834.
2. Gut, I.G. DNA Analysis by MALDI-TOF Mass Spectrometry. *Hum Mutat* **2004**, *23*, 437–441.
3. Clark, A.E.; Kaleta, E.J.; Arora, A.; Wolk, D.M. Matrix-Assisted Laser Desorption Ionization-Time of Flight Mass Spectrometry: A Fundamental Shift in the Routine Practice of Clinical Microbiology. *Clin Microbiol Rev* **2013**, *26*, 547–603, doi:10.1128/CMR.00072-12.
4. Tanaka, K. The Origin of Macromolecule Ionization by Laser Irradiation (Nobel Lecture). In Proceedings of the Angewandte Chemie - International Edition; Wiley-VCH Verlag, August 25 2003; Vol. 42, pp. 3860–3870.
5. Tanaka, K.; Waki, H.; Ido, Y.; Akita, S.; Yoshida, Y.; Yoshida, T. *Protein and Polymer Analyses up to M_z 100 000 by Laser Ionization Time-of-Flight Mass Spectrometry*; 1988; Vol. 2;.
6. CORRESPONDENCE *Laser Desorption Ionization of Proteins with Molecular Masses Exceeding 10 000 Daltons*;
7. Watanabe, T.; Kawasaki, H.; Yonezawa, T.; Arakawa, R. Surface-Assisted Laser Desorption/Ionization Mass Spectrometry (SALDI-MS) of Low Molecular Weight Organic Compounds and Synthetic Polymers Using Zinc Oxide (ZnO) Nanoparticles. *Journal of Mass Spectrometry* **2008**, *43*, 1063–1071, doi:10.1002/jms.1385.
8. Song, K.; Cheng, Q. Desorption and Ionization Mechanisms and Signal Enhancement in Surface Assisted Laser Desorption Ionization Mass Spectrometry (SALDI-MS). *Appl Spectrosc Rev* **2020**, *55*, 220–242.
9. Chiang, C.K.; Chen, W.T.; Chang, H.T. Nanoparticle-Based Mass Spectrometry for the Analysis of Biomolecules. *Chem Soc Rev* **2011**, *40*, 1269–1281, doi:10.1039/c0cs00050g.
10. Law, K.P.; Larkin, J.R. Recent Advances in SALDI-MS Techniques and Their Chemical and Bioanalytical Applications. *Anal Bioanal Chem* **2011**, *399*, 2597–2622.
11. Lim, A.Y.; Ma, J.; Boey, Y.C.F. Development of Nanomaterials for SALDI-MS Analysis in Forensics. *Advanced Materials* **2012**, *24*, 4211–4216, doi:10.1002/adma.201200027.
12. Kang, H.; Yun, H.; Lee, S.W.; Yeo, W.S. Analysis of Small Biomolecules and Xenobiotic Metabolism Using Converted Graphene-like Monolayer Plates and Laser Desorption/Ionization Time-of-Flight Mass Spectrometry. *Talanta* **2017**, *168*, 240–245, doi:10.1016/j.talanta.2017.03.046.
13. Su, C.L.; Tseng, W.L. Gold Nanoparticles as Assisted Matrix for Determining Neutral Small Carbohydrates through Laser Desorption/Ionization Time-of-Flight Mass Spectrometry. *Anal Chem* **2007**, *79*, 1626–1633, doi:10.1021/ac061747w.
14. Cha, S.; Song, Z.; Nikolau, B.J.; Yeung, E.S. Direct Profiling and Imaging of Epicuticular Waxes on *Arabidopsis Thaliana* by Laser Desorption/Ionization Mass Spectrometry Using Silver Colloid as a Matrix. *Anal Chem* **2009**, *81*, 2991–3000, doi:10.1021/ac802615r.
15. Kurita, M.; Arakawa, R.; Kawasaki, H. Silver Nanoparticle Functionalized Glass Fibers for Combined Surface-Enhanced Raman Scattering Spectroscopy (SERS)/Surface-Assisted Laser Desorption/Ionization (SALDI) Mass Spectrometry: Via Plasmonic/Thermal Hot Spots. *Analyst* **2016**, *141*, 5835–5841, doi:10.1039/c6an00511j.
16. Hinman, S.S.; Chen, C.Y.; Duan, J.; Cheng, Q. Calcinated Gold Nanoparticle Arrays for On-Chip, Multiplexed and Matrix-Free Mass Spectrometric Analysis of Peptides and Small Molecules. *Nanoscale* **2016**, *8*, 1665–1675, doi:10.1039/c5nr06635b.
17. Gan, J.; Wei, X.; Li, Y.; Wu, J.; Qian, K.; Liu, B. Designer SiO₂@Au Nanoshells towards Sensitive and Selective Detection of Small Molecules in Laser Desorption Ionization Mass Spectrometry. *Nanomedicine* **2015**, *11*, 1715–1723, doi:10.1016/j.nano.2015.06.010.
18. Du, M.; Chen, D.; Chen, Y.; Huang, Y.; Ma, L.; Xie, Q.; Xu, Y.; Zhu, X.; Chen, Z.; Yin, Z.; et al. Plasmonic Gold Nanoshell-Assisted Laser Desorption/Ionization Mass Spectrometry for Small-Biomolecule Analysis and Tissue Imaging. *ACS Appl Nano Mater* **2022**, *5*, 9633–9645, doi:10.1021/acsanm.2c01850.
19. Seong, B.; Bock, S.; Hahm, E.; Huynh, K.H.; Kim, J.; Lee, S.H.; Pham, X.H.; Jun, B.H. Synthesis of Densely Immobilized Gold-assembled Silica Nanostructures. *Int J Mol Sci* **2021**, *22*, 1–13, doi:10.3390/ijms22052543.
20. Bock, S.; Choi, Y.S.; Kim, M.; Yun, Y.; Pham, X.H.; Kim, J.; Seong, B.; Kim, W.; Jo, A.; Ham, K.M.; et al. Highly Sensitive Near-Infrared SERS Nanoprobes for in Vivo Imaging Using Gold-Assembled Silica Nanoparticles with Controllable Nanogaps. *J Nanobiotechnology* **2022**, *20*, doi:10.1186/s12951-022-01327-7.
21. Tang, H.W.; Ng, K.M.; Lu, W.; Che, C.M. Ion Desorption Efficiency and Internal Energy Transfer in Carbon-Based Surface-Assisted Laser Desorption/Ionization Mass Spectrometry: Desorption Mechanism(s) and the Design of SALDI Substrates. *Anal Chem* **2009**, *81*, 4720–4729, doi:10.1021/ac8026367.

22. Stober, W.; Fink, A.; Ernst Bohn, D. *Controlled Growth of Monodisperse Silica Spheres in the Micron Size Range* 1; 1968; Vol. 26;
23. Lee, J.; Lee, J.; Chung, T.D.; Yeo, W.S. Nanoengineered Micro Gold Shells for LDI-TOF Analysis of Small Molecules. *Anal Chim Acta* **2012**, *736*, 1–6, doi:10.1016/j.aca.2012.05.040.
24. Wu, H.P.; Su, C.L.; Chang, H.C.; Tseng, W.L. Sample-First Preparation: A Method for Surface-Assisted Laser Desorption/Ionization Time-of-Flight Mass Spectrometry Analysis of Cyclic Oligosaccharides. *Anal Chem* **2007**, *79*, 6215–6221, doi:10.1021/ac070847e.
25. Chen, R.; Xu, W.; Xiong, C.; Zhou, X.; Xiong, S.; Nie, Z.; Mao, L.; Chen, Y.; Chang, H.C. High-Salt-Tolerance Matrix for Facile Detection of Glucose in Rat Brain Microdialysates by Maldi Mass Spectrometry. *Anal Chem* **2012**, *84*, 465–469, doi:10.1021/ac202438a.
26. Wen, X.; Dagan, S.; Wysocki, V.H. Small-Molecule Analysis with Silicon-Nanoparticle-Assisted Laser Desorption/Ionization Mass Spectrometry. *Anal Chem* **2007**, *79*, 434–444, doi:10.1021/ac061154l.

Disclaimer/Publisher's Note: The statements, opinions and data contained in all publications are solely those of the individual author(s) and contributor(s) and not of MDPI and/or the editor(s). MDPI and/or the editor(s) disclaim responsibility for any injury to people or property resulting from any ideas, methods, instructions or products referred to in the content.